Desalination and Water Treatment
www.deswater.com
doi: 10.5004/dwt.2018.22041

109 (2018) 45–52
March

Synthesis of AgCl/PES hybrid membranes and their application in removing iodide ion

Fengqin Yu, Haizeng Wang*

Key Laboratory of Marine Chemistry Theory and Technology, Ministry of Education, College of Chemistry and Chemical Engineering, Ocean University of China, Qingdao, Shandong 266100, China, emails: haizwang@ouc.edu.cn (H. Wang), yu1110@126.com (F. Yu)

Received 23 December 2017; Accepted 9 February 2018

ABSTRACT

AgCl/PES hybrid membrane adsorbents with different AgCl contents for iodide ion were prepared by in situ synthesized phase inversion method. Scanning electron microscopy and X-ray diffraction (XRD) analysis confirmed the presence of silver chloride on the hybrid membrane adsorbent. Brunauer, Emmett, and Teller adsorption/desorption found that the membranes have the same isotherm type, but the adsorbed quantity increased with the content of the AgCl. The kinetics of iodide adsorption exhibited that the rate-limiting step may be chemical sorption between sorbent and sorbate. The composite adsorbents used in this study have been proved to be an effective iodide adsorbent with a biggest adsorption capacity of 551 mg g^{-1}. Fourier transform infrared spectroscopy and XRD analyses for the membrane after reaction with iodide confirmed that chloride was exchanged with iodide to form AgI(s). This study can provide a promising method to address radioactive I^- pollution in water.

Keywords: In situ formation; Membrane; Adsorption; Iodide

1. Introduction

Excessive iodide ions in environment have negative impacts on lives living within the ecosystem, because iodide ions take part in the metabolism process of thyroid gland and superfluous iodide ions may damage the growing and brain-developing processes of animals [1]. Besides, radioactive iodine isotopes, ^{129}I, ^{127}I, ^{131}I, etc. which derived from nuclear reactions may contaminate soil and groundwater without appropriate treatment. Once they were released into environment, especially ^{129}I, with a half-life of 1.57×10^7 years, would cause a long-term damage [2,3]. Therefore, effectively preventing the spread of the radioactive iodide ion wastes is quite important, while emergency handling with radioactive iodide in the nuclear dump and polluted water source still is a great challenge around the world [4]. In some natural waters such as salt lakes, iodide is one of the useful natural resources whose extraction is of great importance. The development of a facile method for removing iodine is an important area of research. Various adsorbents have recently been used to adsorb iodide anions from water, such as compounds containing Bi^{3+} [5,6], Hg^{2+} [7], Cu^+ [8] and Pb^{2+}. However, these compounds displayed relatively low adsorption capacities and potential toxicity. Remarkably, AgCl has shown better iodide adsorption ability, and most of the adsorption processes are through chemical adsorption [9]. It is hard to prepare the AgCl particle with small-size and equal distribution because of the characteristic of easy-resolving and reuniting of AgCl under the light.

The difficulty of uniform dispersion microparticles, which was attributed to the high viscosity of the casting solution and the prone agglomeration of microparticles in casting solution, leads to defects and further loose of the materials [10,11]. There have been some reports about adsorption of iodide using spheres including AgCl and as the adsorption-active agents and calcium alginate as the matrix material [12]. Membrane adsorption has the advantages of membrane technology and adsorption technology, which provides a new effective means for biological separation, separation of organic systems and safety of drinking water [13]. In the last decades, affinity membranes have been widely applied in the purification of protein due to its low pressure drop,

* Corresponding author.

fast binding rate, high productivity and easy scale-up [14,15]. Organic–inorganic hybrid membranes can be fabricated most commonly by solution blending method, in situ polymerization and sol–gel method [16].

In this paper, a new method was presented to prepare homogeneous organic–inorganic hybrid AgCl/PES membranes by directly adding silver nitrate ($AgNO_3$) into the polyethersulfone (PES) casting solution via phase inversion process and NaCl solution (2 mol L^{-1}) was used for coagulation bath. The in situ synthesis method solves the problem of easy agglomeration when AgCl particles are formed. On the other hand, it extends the use range of AgCl particles and reduces the photodegradation of AgCl to some extent.

In the process of the membranes coagulation in NaCl bath, $AgNO_3$ in the casting solution reacted with NaCl in the coagulation bath and AgCl particles were obtained in the hybrid membranes. The casting solution was prepared at 60°C for dissolution of PES and $AgNO_3$ in N,N-dimethylacetamide (DMAc) with full stirring overnight in an airtight container, then the clear solution was poured onto a clean glass plate with a slit thickness of 100 μm at room temperature. Then, the solution on the glass was immediately immersed in NaCl bath. After complete coagulation, the membranes were washed in flowing water to remove excess organic solvent and NaCl, finally the membranes were dried in air at room temperature.

2. Materials and methods

2.1. Preparation of membrane adsorbents

All chemicals were obtained from commercial sources and used without further purification unless otherwise specified. The $AgNO_3$ and PES were dissolved in DMAc with 60°C stirring overnight in an airtight container. After all bubbles disappeared, the solution was poured onto a clean glass plate with a casting thickness of 100 μm. Then, the cast film was put into the bath NaCl solution (2 mol L^{-1}) and coagulated. The concentration of NaCl in coagulation bath was set as 2 mol L^{-1} because when the concentration is larger, the diffusion rate is too fast leading to particles agglomeration, and when it is smaller, AgCl will precipitate in the coagulation bath. After complete coagulation, the membranes were washed with DI water until all the NaCl solution was removed and no Cl^- ion was detected.

With different dosage of $AgNO_3$ added into the casting solution, a series of membranes with different composition were prepared. The ratios of $AgNO_3$ and PES in the casting solution are listed in Table 1. The membranes prepared were marked as M0, M1, M2, M3, M4 and M5. The film liquid was ultrasounded for 1 h to make the particles disperse more evenly. The final AgCl content in membranes was measured by resolving the membrane in *N*,*N*-dimethylacetamide and washed by *N*,*N*-dimethylacetamide several times. Then, it was separated and weighed to determine the final AgCl content.

2.2. Characterization of membrane

The surface morphology and the cross-sectional structure of the membranes with different composition were analyzed by scanning electron microscopy (SEM; S-4800, Hitachi, Japan). Before analyzing, the membrane samples were dried overnight, cut into appropriate size, mounted on brass plates, and then sputter coated with gold. The SEM images of the top surface and cross-section morphologies of prepared membranes are shown in Figs. 1 and 2.

Table 1
Composition of casting solutions of the membranes

Membrane	Casting solution composition (wt%)			AgCl content (wt%)
	PES	DMAc	$AgNO_3$:PES (w/w)	
M0	24	76	0	0
M1	24	76	0.01	0.9
M2	24	76	0.1	9
M3	24	76	0.2	15
M4	24	76	0.3	22
M5	24	76	0.4	28

The membrane samples were characterized by specific surface area analyzer (NOVA 2200e, Quantachrome, USA) at liquid nitrogen temperature. Based on the Brunauer, Emmett and Teller (BET) and Barret, Joyner and Halenda (BJH) models, parameters of specific surface area were identified to analyze the pore structures of the membrane adsorbents [17].

The surface crystalline structures of the membranes were characterized by using an X-ray diffraction technique (XRD-6000, Shimadzu). The X-ray diffractograms were taken using Cu K radiation with X-ray scan speed of 2° min^{-1} in the range of 5°–70°. The membranes marked as M1–M5 were all investigated by X-ray diffraction (XRD).

2.3. Adsorption studies

All the sorption experiments were conducted by adding the membranes into airtight bottles containing the iodide solution. The concentration of iodide ions in the solutions was determined using a selective electrode for iodide ion [18].

2.3.1. Adsorption isotherm

In the adsorption isotherm experiment, iodide solutions with various concentrations were prepared. And 0.1 g membrane adsorbent was added into 50 mL iodide solutions. The mixture solutions were shaken on a rotary shaker at 25°C for 24 h. The final iodide concentration in the solution was measured by a selective electrode for iodide ion. The pH was controlled at 5.4–6.0.

2.3.2. Measurement of adsorption kinetics

The kinetics of iodide ions adsorption by AgCl/PES membrane are plotted for different initial iodide ion concentrations of 50, 100 and 150 mg L^{-1} at 25°C. In order to investigate the mechanism of adsorption and determine the rate-controlling step, the pseudo-second-order kinetic model is used to test the experimental data.

The pseudo-second-order kinetic model is represented by the following equation:

$$\frac{t}{q_t} = \frac{1}{K_2 q_e^2} + \frac{1}{q_e} t \tag{1}$$

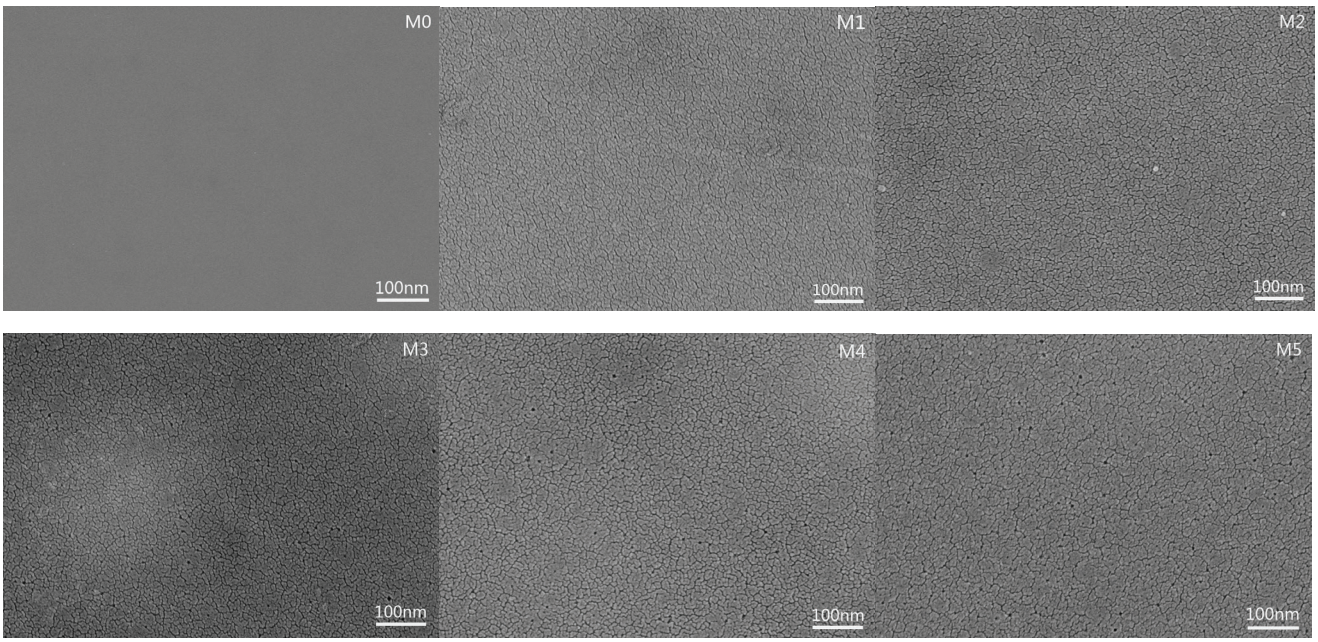

Fig. 1. The SEM images of the top surface of the membranes.

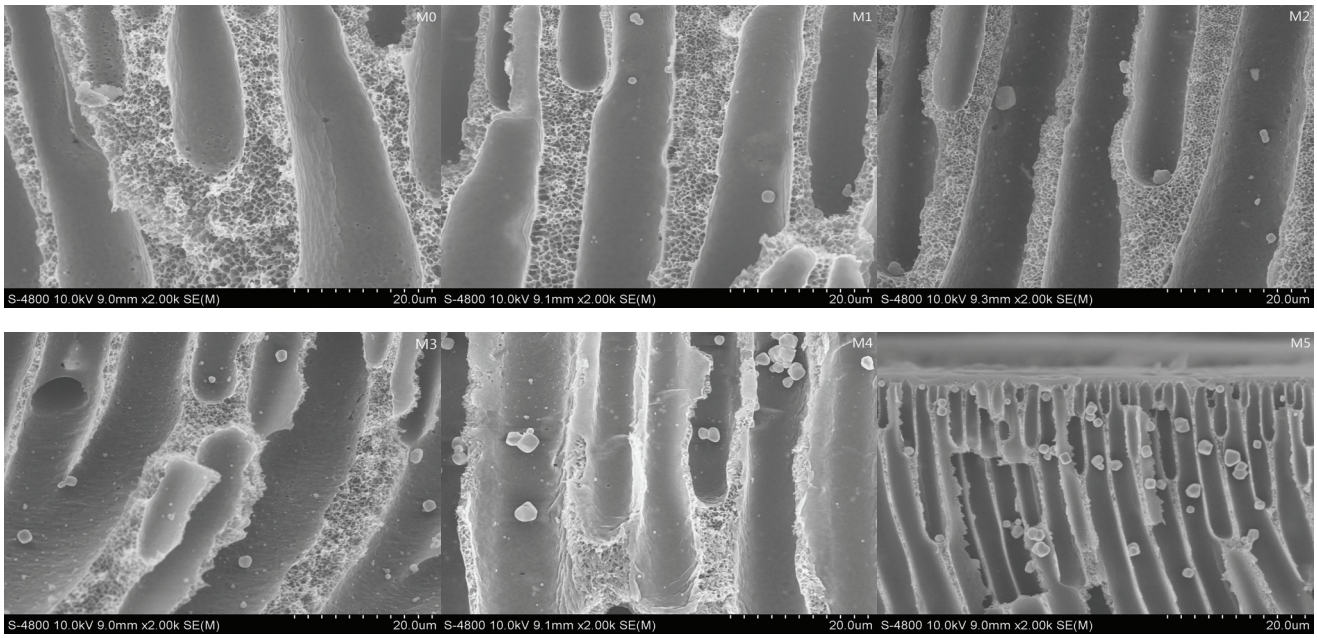

Fig. 2. The SEM images of the cross-section morphologies of the membranes.

where K_2 (g mg^{-1} min^{-1}) is the second-order rate constant, q_t (mg g^{-1}) represents the adsorption capacity at t (min). The equilibrium adsorption capacity (q_e) and the pseudo-second-order rate constants K_2 are obtained from the slope and intercept of the plots of t/q_e against t.

2.3.3. The effect of pH on adsorption

The same procedure was followed as the adsorption isotherm experiment, except that the pH was varied from 2 to 13. The effect of pH on the adsorption was investigated by adjusting the pH with 0.1 mol L^{-1} HCl or NaOH. We choose M3 as the represent to invest the effect of pH on the adsorption.

2.4. Interaction of membrane and iodide

Fourier transform infrared spectroscopy (FTIR) was used to elucidate the interaction of the AgCl/PES blend membrane and iodide. The spectra were collected within the range of wave-number of 400–4,000 cm^{-1}. The specimens were first mixed with potassium bromide and then ground in an agate

mortar (Merck, Germany) at an approximate ratio of 1/100 for the preparation of samples (weight of 0.1 g). The resulting mixture was pressed at 10 t (tons of force) for 5 min. Then, 16 scans and 4 cm^{-1} resolutions were applied in recording the spectra. The background obtained from the scan of pure potassium bromide was automatically subtracted from the sample spectra. All spectra were plotted using the same scale on the absorbance axis.

XRD measurements were conducted to examine the crystalline change of the hybrid membrane before and after adsorption for M3. The X-ray diffractograms were taken using Cu K radiation with X-ray scan speed of 2° min^{-1} in the range of 5°–70°.

3. Results and discussion

3.1. Characterization of membrane

3.1.1. Surface morphology and cross-sectional structure

As shown in Figs. 1 and 2, with the increase of the mass percentage of $AgNO_3$ in the casting solution, the number and size of the pores on the membranes surface are increased, incorporate with the increase of AgCl particles in the channels of the hybrid membranes. AgCl particles are equally distributed in the hybrid membranes. The number of AgCl particles formed in membrane increased, while the increasing of concentration of $AgNO_3$ in the casting solution from the membrane sectional microstructure (Fig. 2).

3.1.2. Pore structure of the membrane

To further characterize the pore structure of the membrane, membranes M1, M3 and M5 were analyzed as representative by BET analysis. The nitrogen adsorption/desorption isotherm is shown in Fig. 3 and the pores size distribution curve (inset) from adsorption isotherm of M1, M3 and M5 using BJH method. From the isothermal curves is shown in Fig. 4. It can be found that the three membranes have the same isotherm type, but the adsorbed quantity increased with the content of the AgCl. When $P/P_0 > 0.80$, a large increase in volume (the take-off on the curve) is observed, which suggests that there is a large amount of macropores in the samples [19]. Furthermore, M5 has larger average pore width and exhibits higher BET surface area of 9.70 $m^2 g^{-1}$ than M3 found to be 7.19 $m^2 g^{-1}$ and M1 6.87 $m^2 g^{-1}$.

3.1.3. X-ray diffraction of the membranes

XRD patterns (Fig. 5) of the membranes show no big difference, only minor changes in relative intensity of some characteristic peaks without variation in the peak positions. It further verifies that AgCl does not exist in the form of Ag or Ag_2O, which is not agreeing with the results in other literatures [20,21]. It means that AgCl formed in the membrane after the phase inversion and it did not photodegrade as the absence of Ag or Ag_2O.

3.2. Adsorption studies

3.2.1. Adsorption isotherm

From the adsorption isotherm experiment, we can see that the different membranes marked as M0–M5 can reach

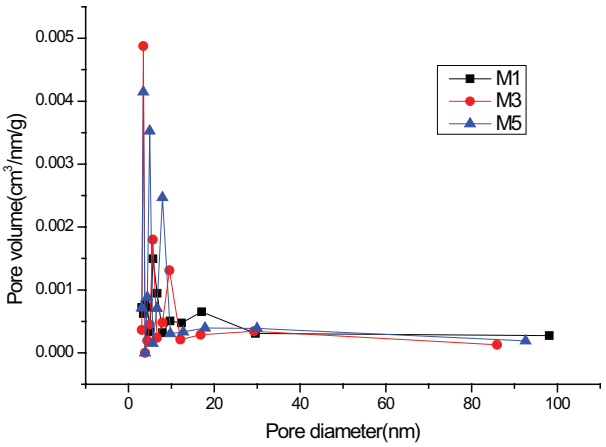

Fig. 4. The pore diameter distribution of the membranes.

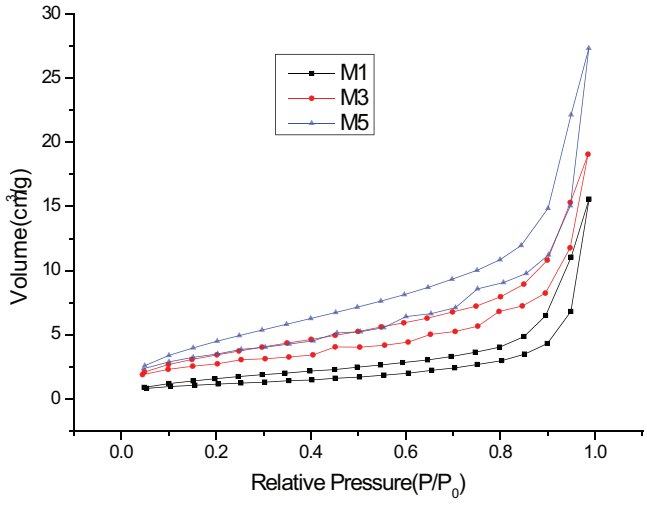

Fig. 3. N_2 adsorption isotherms of M1, M3, M5.

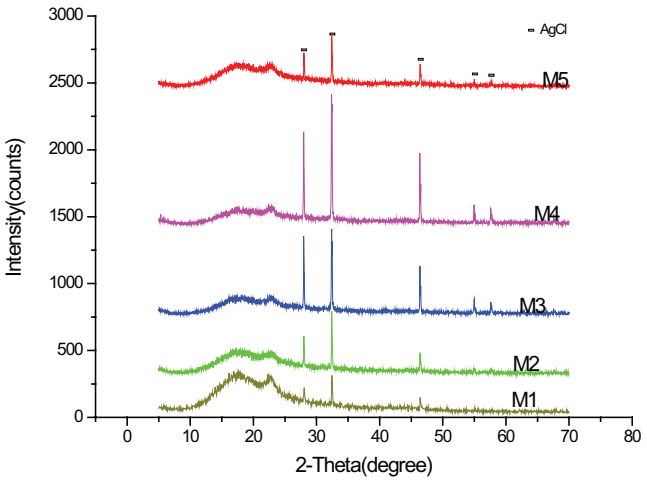

Fig. 5. XRD patterns of M1–M5.

the adsorption capacities of 0, 80, 140, 224, 327 and 551 mg g^{-1} at 25°C (Fig. 6). Hence, the composite membrane adsorbents have higher adsorption capacity compared with the materials in articles [12]. The results showed that this material has a very good adsorption capacity for iodide ion. The adsorption isotherms are of H2 type, proving that the adsorption is chemical adsorption. To further research the highest adsorption capacity of material for iodide ion, we make model fitting of Langmuir and Freundlich for adsorption isotherm.

The Langmuir modified model is:

$$\frac{C_e}{q_e} = \frac{1}{K_L q_m} + \frac{C_e}{q_m} \tag{2}$$

In this model, q_e (mg g^{-1}) is for the adsorption capacity of composite membrane for iodide ion under equilibrium condition. q_m (mg g^{-1}) is for the limitation adsorption capacity of composite for iodide ion. K_L is adsorption constant.

The Freundlich modified model is:

$$\ln q_e = \ln K_f + \frac{1}{n} \ln C_e \tag{3}$$

In this model, q_e (mg g^{-1}) is for the adsorption capacity of composite membrane for iodide ion under equilibrium condition. q_m (mg g^{-1}) is for the limitation adsorption capacity of composite for iodide ion. K_f and n are characteristic adsorption constant.

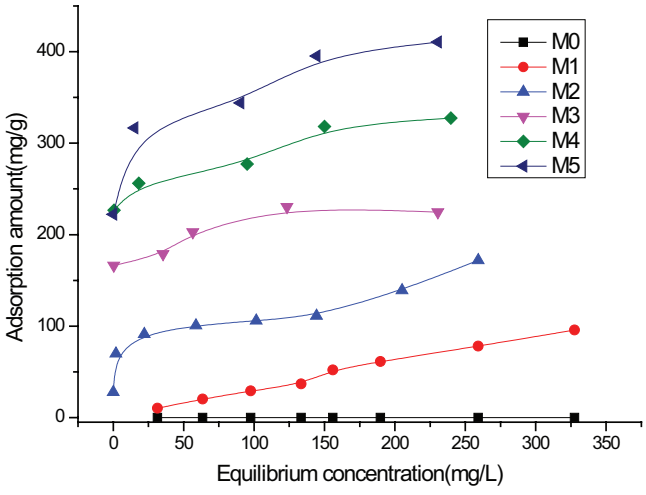

Fig. 6. Adsorption isotherm of membranes.

From the result (Table 2), adsorption of M1 membrane is most consistent to the Freundlich model without saturation adsorption capacity. M2–M5 are consistent to Langmuir model with 131.5, 232.6, 333.3 and 454.5 mg g^{-1} of limitation adsorption capacity, respectively. These membranes have high adsorption capacity for iodide ion.

3.2.2. The kinetics of iodide ion adsorption

Three batch adsorption experiments with different iodide concentrations were conducted to study the adsorption kinetics of iodide onto the AgCl/PES membrane. In the experiments, initial pH was 5.6. As shown in Fig. 7, most of iodide adsorption on the membrane rapidly occurs in the first 1.5 h, followed by a relatively slow process. The adsorption equilibrium was reached at about 100 min (M1) and 600 min (M3 and M5).

The plot t/q_t vs. t for various iodide concentrations are shown in Figs. 7(d)–(f) and the pseudo-second-order adsorption rate constants for different initial concentrations are summarized in Table 3. As we know, chemical adsorption is dominant in iodide adsorption of AgCl/PES membrane, and the linear regression coefficients R^2 and pseudo-second-order adsorption rate constants at different initial concentrations and different membrane adsorbents is shown in Table 3. As displayed in Fig. 7 and Table 3, the estimated equilibrium adsorption capacities at 50, 100 and 150 mg L^{-1} are in good agreement with the experimental results. The pseudo-second-order model, based on the assumption that the rate-limiting step may be chemical sorption between sorbent and sorbate [22] provides the best correlation of the data.

3.2.3. The effect of pH on iodide adsorption

The concentration of solution was determined after adding M3 (0.1 g) into solution and then shaking for 24 h at 25°C to calculate the adsorbing capacity with changing of pH. The result is shown as Fig. 8. The result shows that the adsorbing capacity of membrane does not change while changing the pH. This reflects that this membrane can be applied into acid stage, alkaline and neutral conditions with wide application.

3.2.4. Crystal structures analysis of the membrane

XRD measurements were conducted to examine the crystalline change of the hybrid membrane in the absence of the inorganic particles before and after adsorption as shown in Fig. 9. All the diffraction peaks before adsorption are indexed to AgCl and no other crystalline is detected. It means that AgCl formed in the membrane after the phase inversion

Table 2
Langmuir and Freundlich fitting constant for adsorption isotherm

No.	Langmuir			Freundlich		
	q_m	K_L	R^2	K_f	n	R^2
M1	2,000	0.00015	0.0262	2.87	1.024	0.992
M2	131.5	0.10	0.969	61.56	7.057	0.955
M3	232.6	0.21	0.997	167.33	20.20	0.744
M4	333.3	0.16	0.995	175.91	8.28	0.650
M5	454.5	0.075	0.995	295.30	15.17	0.837

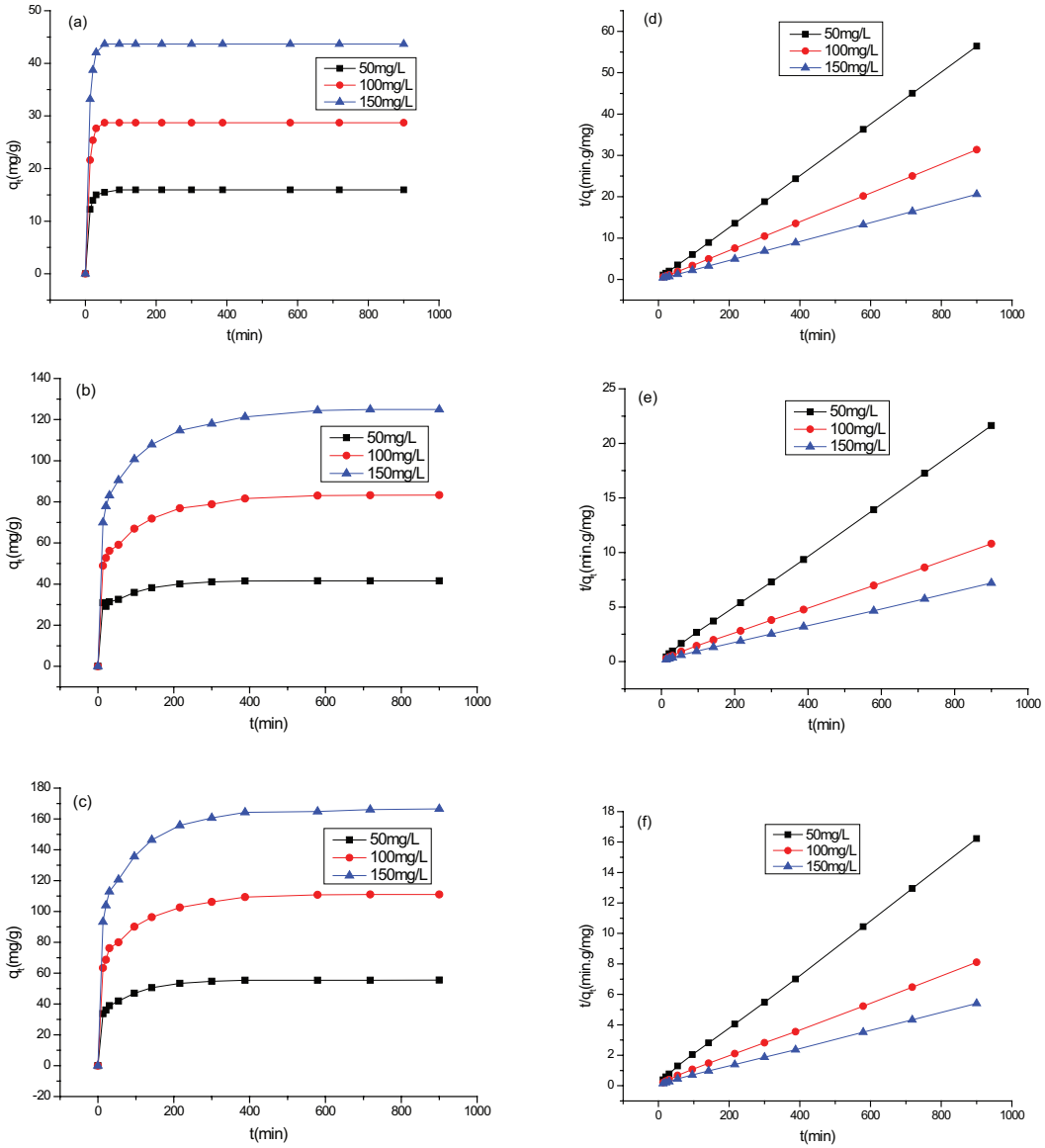

Fig. 7. Adsorption kinetics curves of M1 (a), M3 (b) and M5 (c) for iodide ion, pseudo-second-order kinetics model for iodide ion adsorption on the M1 (d), M3 (e) and M5 (f).

Table 3
Pseudo-second-order adsorption rate constants at different initial concentrations and different adsorbed amount

	C_0 (mg L^{-1})	K_2 (g/mg min)	R^2	$q_{e,cal}$ (mg g^{-1})
M1	50	0.037	0.9999	16
	100	0.026	0.9999	28.7
	150	0.018	0.9998	43.7
M3	50	0.0057	0.9998	42.2
	100	0.00061	0.9997	85.5
	150	0.00039	0.9998	128.2
M5	50	0.0013	0.9998	56.5
	100	0.00047	0.9997	113.6
	150	0.00034	0.9997	169.5

and it did not photodegrade as the absence of Ag or Ag_2O. The XRD after adsorption shows that diffraction peaks are indexed to AgCl and AgI which indicates that some of AgCl particles reacted with iodide ion and generated AgI.

3.2.5. Interaction of membrane and iodide

To explore the interaction mechanism between the membrane and the adsorbed iodide, FTIR spectroscopy analysis was conducted. As mentioned in the adsorption isotherm study, the removal of iodide from water by the membrane adsorbent may be mainly due to the adsorption of iodide onto the AgCl particle encapsulated in membrane. Hence, FTIR spectroscopy analysis on membrane before and after the adsorption of iodide were performed to illustrate the potential interaction between AgCl and the adsorbed iodide and M3 was chosen

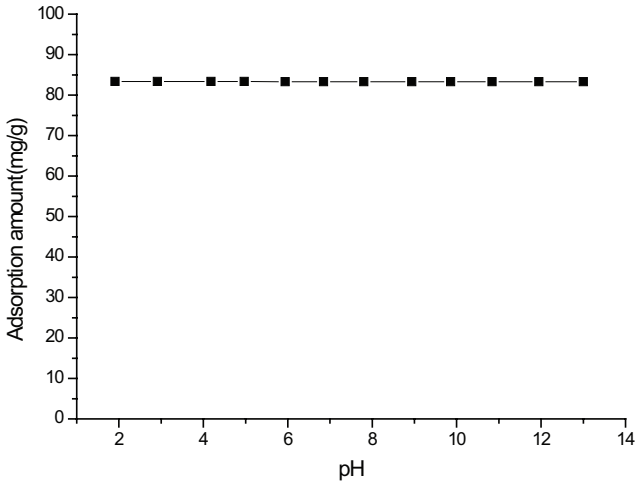

Fig. 8. The effect of pH on iodide adsorption.

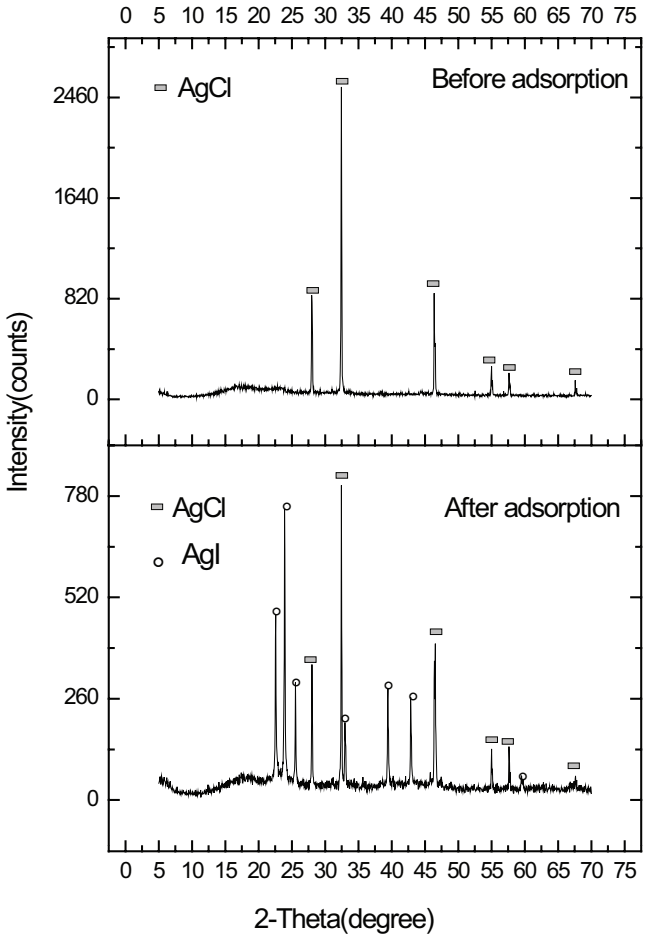

Fig. 9. The X-ray diffraction (XRD) patterns of the M3 before and after adsorption.

as represent since all the membranes have the same law. The FTIR results shown in Fig. 10 reveal the changes in the absorption bands of the surface functional groups of AgCl due to the iodide adsorption. FTIR spectra of membrane adsorbed iodide ion created a new absorption peak at 1,384.8 cm^{-1} which may

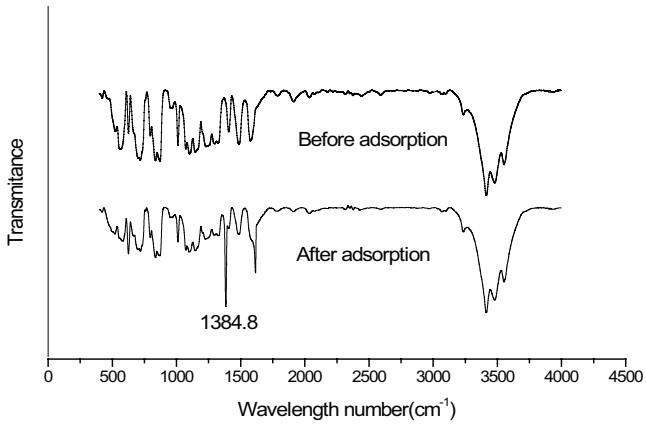

Fig. 10. FTIR spectra of M3 before and after adsorption.

be the peak of AgI, as reported by Zhai et al. [23]. So we can predict that AgI was produced during the adsorption process corresponding with the FTIR results.

4. Conclusion

AgCl/PES composite membrane adsorbents for iodide have been prepared via in situ formation. The AgCl particles distributed evenly in the membranes and increase as the increase of the $AgNO_3$ amount in the casting solution.

The iodide adsorbed quantity increased with the content of the AgCl cooperated with the N_2 adsorption/desorption isotherm.

The experimental kinetic data can be fitted by pseudo-second-order model quite well. Chemical adsorption is dominant in iodide adsorption of AgCl/PES membrane.

The adsorption amount is insensitive to solution pH. The prepared composite adsorbents have a high adsorption capacity. They are very suitable for the adsorption of iodide form aqueous solutions. The adsorption isotherms are of H2 type, proving that the adsorption is chemical adsorption. The comparison of XRD patterns and FTIR of the composite adsorbents before and after adsorption shows that AgCl in the original adsorbents changes into AgI after adsorption, confirming the chemical nature of the adsorption.

Acknowledgement

This work was supported by Shandong province independent innovation major special plan, China (Grant No. 931248050).

References

[1] P. Lind, W. Langsteger, M. Molnar, H.J. Gallowitsch, P. Mikosch, I. Gomez, Epidemiology of thyroid diseases in iodine sufficiency, Thyroid, 8 (1998) 1179–1183.
[2] Q. Hu, P. Zhao, J.E. Moran, J.C. Seaman, Sorption and transport of iodine species in sediments from the Savannah River and Hanford Sites, J. Contam. Hydrol., 78 (2005) 185–205.
[3] S.D. Park, J.S. Kim, S.H. Han, Y.K. Ha, K.S. Song, K.Y. Jee, The measurement of ^{129}I for the cement and the paraffin solidified low and intermediate level wastes (LILWs), spent resin or evaporated bottom from the pressurized water reactor (PWR) nuclear power plants, Appl. Radiat. Isot., 67 (2009) 1676–1682.

[4] P. Mao, B. Qi, Y. Liu, L. Zhao, Y. Jiao, Y. Zhang, J. Zheng, Q. Li, J.F. Wang, S. Chen, Y. Yang, Ag^{II} doped MIL-101 and its adsorption of iodine with high speed in solution, J. Solid State Chem., 237 (2016) 274–283.
[5] L. Liu, W. Liu, X. Zhao, D. Chen, R. Cai, W. Yang, S. Komarneni, D. Yang, Selective capture of iodide from solutions by microrosette-like δ-Bi_2O_3, ACS Appl. Mater. Interfaces, 6 (2014) 16082–16090.
[6] H. Kodama, Removal of iodide ion from simulated radioactive liquid waste, Czech. J. Phys., 49 (1999) 971–977.
[7] S.D. Balsley, P.V. Brady, J.L. Krumhansl, H.L. Anderson, Iodide retention by metal sulfide surfaces, cinnabar and chalcocite, Environ. Sci. Technol., 30 (1996) 3025–3027.
[8] G. Lefèvre, J. Bessière, J.J. Ehrhardt, A. Walcarius, Immobilization of iodide on copper(I) sulfide minerals, J. Environ. Radioact., 70 (2003) 73–83.
[9] T. Karanfil, E.C. Moro, S.M. Serkiz, Development and testing of a silver chloride-impregnated activated carbon for aqueous removal and sequestration of iodide, Environ. Technol., 26 (2005) 1255–1262.
[10] K.H. Chan, E.T. Wong, A. Idrisa, N.M. Yusof, Modification of PES membrane by PEG-coated cobalt doped iron oxide for improved Cu(II) removal, J. Ind. Eng. Chem., 27 (2015) 283–290.
[11] M.K. Sinha, M.K. Purkait, Increase in hydrophilicity of polysulfone membrane using polyethylene glycol methyl ether, J. Membr. Sci., 437 (2013) 7–16.
[12] H. Zhang, T. Guo, Q. Li, X. Ye, Z. Wu, Iodide adsorption onto three organic-inorganic composite adsorbents, Adsorpt. Sci. Technol., 30 (2012) 449–460.
[13] E.N. Lightfoot, T.W. Root, J.L. O'Dell, Emergence of ideal membrane cascades for downstream processing, Biotechnol. Progr., 24 (2008) 599–605.
[14] C.I. Chen, Y.M. Ko, W.L. Lien, Y.H. Lin, I.T. Li, C.H. Chen, C.J. Shieh, Y.C. Liu, Development of the reversible PGA immobilization by using the immobilized metal ion affinity membrane, J. Membr. Sci., 401 (2012) 33–39.
[15] G. Serpa, E.F. Augusto, W.M. Tamashiro, M.B. Ribeiro, E.A. Miranda, S.M.A. Bueno, Evaluation of immobilized metal membrane affinity chromatography for purification of an immunoglobulin G1 monoclonal antibody, J. Chromatogr. B, 816 (2005) 259–268.
[16] Z. Xu, L. Yu, L. Han, Polymer-nanoinorganic particles composite membranes: a brief overview, Front. Chem. Eng. China, 3 (2009) 318–329.
[17] J. Zhuang, Physical and Chemistry Experiment, Higher Education Press, China, 2004.
[18] M. Lyczewska, M. Kakietek, K. Maksymiuk, J. Mieczkowski, A. Michalska, Comparison of trihexadecylalkylammonium iodides as ion-exchangers for polyacrylate and poly(vinyl chloride) based iodide-selective electrodes, Sens. Actuators, B, 146 (2010) 283–288.
[19] J. Hou, G. Dong, Y. Ye, V. Chen, Enzymatic degradation of bisphenol-A with immobilized lactase on TiO_2, sol–gel coated PVDF membrane, J. Membr. Sci., 469 (2014) 19–30.
[20] Y.Z. Chen, Y.X. Zhou, H. Wang, J. Lu, T. Uchida, Q. Xu, S.H. Yu, H.L. Jiang, Multifunctional PdAg@MIL-101 for one-pot cascade reactions: combination of host-guest cooperation and bimetallic synergy in catalysis, ACS Catal., 5 (2015) 2062–2069.
[21] N. Mohaghegh, S. Kamrani, M. Tasviri, M. Elahifard, M. Gholami, Nanoporous Ag_2O photocatalysts based on copper terephthalate metal–organic frameworks, J. Mater. Sci., 50 (2015) 4536–4546.
[22] M.Y. Chang, R.S. Juang, Adsorption of tannic acid, humic acid, and dyes from water using the composite of chitosan and activated clay, J. Colloid Interface Sci., 278 (2004) 18–25.
[23] Q.A. Zhai, J.A. Cai, J.A. Li, W. Hu, X. Zhang, A. Geng, Z. Shen, J. Wang, Studies of host-guest nanocomposite material (NaZSM-5)-AgI, Chin. J. Chem. Phys., 18 (2005) 1029–1033.